

Early postnatal switch in GABA_A receptor α -subunits in the reticular thalamic nucleus

Susanne Pangratz-Fuehrer,¹ Werner Sieghart,² Uwe Rudolph,³ Isabel Parada,¹
and John R. Huguenard¹

¹Department of Neurology and Neurological Sciences, Stanford University School of Medicine, Stanford, California; ²Brain Research Institute Vienna, University of Vienna, Vienna, Austria; and ³Laboratory of Genetic Neuropharmacology, McLean Hospital, Mailman Research Center, Harvard Medical School, Belmont, Massachusetts

Submitted 24 September 2015; accepted in final form 2 December 2015

Pangratz-Fuehrer S, Sieghart W, Rudolph U, Parada I, Huguenard JR. Early postnatal switch in GABA_A receptor α -subunits in the reticular thalamic nucleus. *J Neurophysiol* 115: 1183–1195, 2016. First published December 2, 2015; doi:10.1152/jn.00905.2015.—The GABAergic neurons of the thalamic reticular nucleus (nRt) provide the primary source of inhibition within the thalamus. Using physiology, pharmacology, and immunohistochemistry in mice, we characterized postsynaptic developmental changes in these inhibitory projection neurons. First, at postnatal days 3–5 (P3–5), inhibitory postsynaptic currents (IPSCs) decayed very slowly, followed by a biphasic developmental progression, becoming faster at P6–8 and then slower again at P9–11 before stabilizing in a mature form around P12. Second, the pharmacological profile of GABA_A receptor (GABA_AR)-mediated IPSCs differed between neonatal and mature nRt neurons, and this was accompanied by reciprocal changes in α_3 (late) and α_5 (early) subunit expression in nRt. Zolpidem, selective for α_1 - and α_3 -containing GABA_ARs, augmented only mature IPSCs, whereas clonazepam enhanced IPSCs at all stages. This effect was blocked by the α_5 -specific inverse agonist L-655,708, but only in immature neurons. In α_3 (H126R) mice, in which α_3 -subunits were mutated to become benzodiazepine insensitive, IPSCs were enhanced compared with those in wild-type animals in early development. Third, tonic GABA_AR activation in nRt is age dependent and more prominent in immature neurons, which correlates with early expression of α_5 -containing GABA_ARs. Thus neonatal nRt neurons show relatively high expression of α_5 -subunits, which contributes to both slow synaptic and tonic extrasynaptic inhibition. The postnatal switch in GABA_AR subunits from α_5 to α_3 could facilitate spontaneous network activity in nRt that occurs at this developmental time point and which is proposed to play a role in early circuit development.

GABA_AR α_5 ; subunit turnover; IPSCs; tonic current; mouse

THE γ -AMINOBUTYRIC ACID (GABA)-ergic signaling system undergoes significant changes during development. Altered gating kinetics and allosteric modulation lead to functional and pharmacological differences in these receptors (Cherubini and Conti 2001; Macdonald and Olsen 1994; McKernan and Whitington 1996; Mody and Pearce 2004). The developmental switch in the α -subunit expression has been associated with a shift in kinetics of GABA-mediated inhibitory postsynaptic potentials, which become faster in several brain regions within the first 2 postnatal weeks (Hollrigel and Soltesz 1997; Okada et al. 2000; Vicini et al. 2001). This phenomenon of slow GABAergic transmission during early development

may be required to ensure synaptic activation in times of sparse synaptic connectivity (Dunning et al. 1999). On the other hand, studies in the developing hippocampus have shown that GABA-mediated excitation could drive epileptiform activity (Dzhala and Staley 2003; Khalilov et al. 2003). Studies in humans and animal models suggest that mutations or alterations in GABA_A receptor (GABA_AR) subunits might be linked to epilepsy in children (Brooks-Kayal 2005; Brooks-Kayal et al. 1998; Harvey et al. 1997; Swann 2004; Zhang et al. 2004). For example, a hyperthermia model of perinatal seizures is associated with persistent low expression of α_1 -subunit and a smaller amplitude of GABAergic currents (Cossette et al. 2002). A failure in the developmental subunit switch might lead to persistent changes in circuitry that could be pathological, such as in generalized childhood absence epilepsy (AE), which has a strong dependence on proper GABA_AR function (Huguenard and McCormick 2007). Notably, several mutations of GABA_ARs have been associated with AE (Kang and Macdonald 2004; Maljevic et al. 2006; Marini et al. 2003; Tan et al. 2007; Wallace et al. 2001). Absence seizures appear to derive from the intrathalamic network responsible for generation of sleep spindle oscillations (Huguenard and Prince 1994; von Krosigk et al. 1993), although other network substrates are proposed (Leresche et al. 2012; Pinault and O'Brien 2005). In particular, the GABAergic thalamic reticular nucleus (nRt) plays a central role in regulating experimental AE by controlling this form of spindle activity (Avanzini et al. 1993; Huntsman et al. 1999; Sohal and Huguenard 2003). It has been shown that mutant mice lacking functional inhibition within the nRt display hypersynchronous thalamic epileptiform activity and absence-related seizures (DeLorey et al. 1998; Huntsman et al. 1999). In our previous work, we found indications for nRt-specific location of endogenous benzodiazepine (BZ)-binding site ligands (endozepines) (Christian et al. 2013). Synaptic inhibitory responses in nRt are functionally mature at postnatal day 12 (P12) (Huntsman and Huguenard 2000), a stage when thalamic spindle generation is already robust (Jacobsen et al. 2001). However, in neonatal mice younger than P12, a unique pattern of spontaneous giant inhibitory network responses has been observed (Pangratz-Fuehrer et al. 2007). These early network responses, proposed to play a role in circuit formation, depend in part on depolarizing GABA responses but also may rely on the particular GABA_AR composition. Thus GABA_AR within nRt may impact absence seizure susceptibility in the developing brain. Although the specific developmental sequence of

Address for reprint requests and other correspondence: J. R. Huguenard, Dept. of Neurology and Neurological Sciences, Stanford Univ. School of Medicine, Stanford, CA 94305 (e-mail: John.Huguenard@stanford.edu).

GABA_AR expression in humans is not well understood, such changes may explain in part the age-dependent incidence of AE in children (Caraballo and Dalla 2013). In the present study, we used immunohistochemistry, voltage-clamp recordings, and α -subunit-specific pharmacology in wild-type (WT) and mutant mice carrying a BZ-insensitive GABA_AR α_3 -subunit to assess the functional properties of inhibition in the nRt in the period before the spindle-generating circuitry is mature.

MATERIALS AND METHODS

Animals. Wild-type and mutant mice [α_3 (H126R)] pups of either sex were used at P3–20. Mutants were mice homozygous for a histidine-to-arginine point mutation at position 126 of the GABA_AR α_3 -subunit (5–6 backcrosses to the 129/SvJ background) that were generated as described previously (Low et al. 2000). Some confirmatory experiments utilized P5–10 Sprague-Dawley rat pups (Simonsen Laboratories, Gilroy, CA). Experiments were performed in accordance with approved procedures (Protocol 12321/0) established by the Administrative Panel on Laboratory Animal Care at Stanford University. Mice were deeply anesthetized by intraperitoneal injection with pentobarbital (50 mg/kg) until unresponsive and were then decapitated. Brains were blocked, removed, and placed in ice-cold (4°C) oxygen-equilibrated (95% O₂-5% CO₂) “cutting” solution containing (in mM) 234 sucrose, 11 glucose, 24 NaHCO₃, 2.5 KCl, 1.25 NaH₂PO₄, 10 MgSO₄, and 0.5 CaCl₂ for ~1 min. Horizontal slices (200 μ m) were cut with a Vibratome (TPI, St. Louis, MO), hemisected, and incubated in a preheated (32°C) oxygen-equilibrated chamber filled with artificial cerebrospinal fluid (aCSF) containing (in mM) 126 NaCl, 26 NaHCO₃, 10 glucose, 2.5 KCl, 2 MgCl₂·6H₂O, 2 CaCl₂·2H₂O, and 1.25 NaH₂PO₄·H₂O for 1 h before recording.

Electrophysiology. Whole cell patch-clamp recordings were obtained from nRt neurons in brain slices maintained in a chamber with a constant flow of aCSF perfusion (2 ml/min) equilibrated with 95% O₂-5% CO₂. Experiments were conducted at room temperature. Glass electrodes (tip resistance 2.5–3.3 M Ω ; KG-33, borosilicate glass; Garner Glass, Claremont, CA) were pulled in multiple stages using a Flaming-Brown micropipette puller (model P-87; Sutter Instruments, Novato, CA) and filled with high-chloride solution, which contained (in mM) 135 CsCl, 5 lidocaine *N*-ethyl bromide (QX-314), 2 MgCl₂, 10 EGTA (Sigma, St. Louis, MO), and 10 HEPES (Sigma). The solution was adjusted with CsOH to pH 7.3. Voltage-clamp recordings were made from visually identified neurons within nRt using a fixed-stage upright microscope (Axioskop; Zeiss, Thornwood, NY) equipped with a \times 63 objective, Normarski optics, and an infrared-sensitive video camera (Cohu, San Diego, CA). Only one experiment per slice was performed to study pharmacology (*n* slices), whereas up to two cells per slice were recorded to describe developmental changes (*n* cells). With high-chloride intracellular solution, spontaneous inhibitory postsynaptic currents (sIPSCs) were recorded as inward currents at a holding potential of –60 mV. Access resistance of all recorded cells was monitored constantly throughout each experiment. Data were only included in the final analysis if access was <18 M Ω and stable (25% tolerance) for the duration of the experiment.

Pharmacology and method of application. Isolated GABA_AR-mediated IPSCs were recorded in the presence of (\pm)-2-amino-5-phosphonopentanoic acid (APV; 100 μ M; Sigma) and 6,7-dinitroquinoxaline-2,3-dione (DNQX; 20 μ M; RBI, Natick, MA) to block ionotropic glutamate receptors. Concentrated solutions of clonazepam (CZP; 100 μ M; final concentration 100 nM), zolpidem (ZLP; 100 μ M; final concentration 100 nM), L-655,708 (L-655; 15 μ M; final concentration 15 nM), tetrodotoxin (TTX; 1 mM; final concentration 1 μ M), and gabazine (GBZ; 10 mM; final concentrations 10 and 0.2 μ M) (all from Sigma) were stored at 4°C, diluted with aCSF before experiments, and applied via multibarrel local perfusion unless

stated otherwise. The solvent for all stocks except for TTX was DMSO, and drug effects were compared with solvent controls, in which DMSO was diluted to the same final concentration as the drug-containing solution, typically 0.1% (vol/vol).

Data collection and analysis. Data were filtered at 2 kHz, collected, and sorted with locally written software [Metatape, WDetecta, and WinScanSelect (J. R. Huguenard)] and then analyzed using pCLAMP 9 (Axon Instruments, Union City, CA) and Origin (MicroCal Software, Northampton, MA). The following properties of averaged IPSCs (*n* > 50 events/cell) were determined: rise times (the time required to rise from 10 to 90% of peak amplitude), 90% widths (the width at 10% maximum amplitude), half widths, peak current amplitude, frequency, and the weighted decay time constant (τ_{dw}), which was calculated using the following equation: $\tau_{dw} = [(A_{fast} \cdot \tau_{fast} + A_{slow} \cdot \tau_{slow}) / (A_{fast} + A_{slow})]$.

The analysis for tonic current was performed as reported previously (Sipila et al. 2007). Briefly, we calculated an all-points histogram of the recorded voltage-clamp current (>30 s) for each experimental condition either immediately before drug application (control) or at the end of the period of application at which time drug equilibrium was achieved. Gaussian fits were obtained for the histograms, and these were skewed, with IPSCs contributing to a “negative tail” with currents more inward than those occurring between sIPSCs. To minimize the contribution of IPSCs to the fitted Gaussian curves, bins on the negative side of the peak with bins filled to less than half of the peak amplitude were excluded from the analysis (Sipila et al. 2007). In addition, in a separate analysis on a subset of cells, we confirmed that analysis of baseline noise, as measured during IPSC-free periods of recording (Porcello et al. 2003), provided qualitatively similar results, showing increases in baseline noise during GABA application and decreases in the presence of GBZ. All data are means \pm SE. Student's *t*-test was used to assess statistical significance for drug effects, and one-way ANOVA followed by Tukey's post hoc test was used for comparisons between group means unless otherwise stated. Differences were regarded significant if *P* < 0.05. Higher levels of significance are indicated as *P* < 0.01 or *P* < 0.001.

Immunocytochemistry. Animals younger than P5 were deeply anesthetized by intraperitoneal injection with pentobarbital odium (50 mg/kg) until unresponsive and were then decapitated, whereas older mice were anesthetized and then perfused through the ascending aorta with 0.1 M phosphate-buffered saline (PBS; pH 7.4). Brains were removed and placed in 4% paraformaldehyde in 0.1 M PBS (pH 7.4) for 24 h, postfixed in PBS, cryoprotected in 30% sucrose in 0.1 M PBS, and then resectioned in a freezing microtome (HM 400; Microm, Heidelberg, Germany) at 35 μ m.

Immunoperoxidase staining. Sections were reacted with 0.5% H₂O₂ for 30 min to inactivate endogenous peroxidase and then treated with 50% alcohol for 10 min. After being rinsed in PBS, free-floating sections were blocked in 10% normal goat serum and then incubated for 16 h with primary antibodies diluted in PBS and 0.4% Triton X-100 at 4°C. On the following day, sections were rinsed in PBS and incubated in biotinylated secondary antibodies diluted in goat anti-rabbit serum (Vectastain Elite ABC kit; catalog no. PK 6101; Vector Laboratories, Burlingame, CA) for 1 h. After being rinsed in PBS, the sections were incubated with AB reagents from the same ABC kit for 1 h. Finally, the sections were treated with 0.4 mM 3,3'-diaminobenzidine (Sigma) and 0.01% H₂O₂ for 10 min and then mounted on slides and coverslipped with DPX mounting medium (catalog no. 31,761-6; Aldrich) for microscopy.

Immunofluorescence staining. We assessed the distribution of GABA_AR α_3 - and α_5 -subunits and the postsynaptic marker gephyrin in mice from P4–30. For double immunofluorescence of GABA_AR subunit antibodies with single-cell morphology, biocytin (0.05%; Sigma) was included in the internal pipette solution to fill neurons during electrophysiological recordings. Horizontal slices were resectioned at 35 μ m with a freezing microtome, mounted on slides, and processed using the water bath antigen-retrieval method (Jiao et al.

1999). Sections were incubated in 0.05 M sodium citrate solution (pH 9) at room temperature for 30 min and then heated in the same solution for 10 min at 90°C in a microwave oven. Sections were allowed to cool at room temperature and were then incubated with 10% normal goat serum in 0.1 M PBS (pH 7.4), followed by incubation with the primary antibodies and monoclonal mouse gephyrin antibodies (dilution 1:1,000; Alexis Chemicals, San Diego, CA). Sections were incubated in a rotatory shaker overnight at 4°C, rinsed with PBS, and then incubated with fluorescent secondary antibodies (goat anti-mouse Texas red and goat anti-rabbit fluorescein; both from Molecular Probes; 1 μg/ml) for 2 hr. Subsequently, sections were mounted on SuperfrostPlus slides (Fisher Scientific, Houston, TX) and coverslipped. The subcellular location of GABA_AR subunits and the postsynaptic marker gephyrin were then assessed with laser confocal microscopy (LSM 510 confocal laser scanning microscope; Zeiss, Oberkochen, Germany) for double immunofluorescence staining.

RESULTS

Slow IPSCs dominate early GABAergic transmission in nRt. We recorded isolated sIPSCs from nRt neurons in mouse thalamic slices at P3-16 in voltage-clamp mode at -60 mV and in the presence of APV (100 μM) and DNQX (20 μM) to block ionotropic glutamate receptors. Analysis of sIPSC properties revealed significant developmental changes. On the basis of distinct age-dependent sIPSC characteristics, we organized cells into the following four age groups: P3-5, P6-8, P9-11, and P12-15. At P3-5, we recorded spontaneous activity from 61 of 74 cells (82.4% of all neurons); the remaining 13 cells (17.6%) were silent. In four of these silent cells, brief trains of electrical stimulation within nRt triggered subsequent barrages of spontaneous IPSC activity, suggesting that absence of sIPSCs in

some cells was related to low activity levels rather than lack of postsynaptic receptors. Example traces recorded at four different developmental stages show that at P5 (Fig. 1A), sIPSCs occurred at low frequencies with significantly slower decay times compared with all other age groups (mean τ_{dw} at P3-5: 156 ± 8 ms). In contrast, sIPSCs at P6-8 (Fig. 1B) decayed significantly faster (mean τ_{dw} at P6-8: 95.4 ± 5.5 ms, $n = 13$; $P < 0.001$). Surprisingly, at P9-11, sIPSC decay rates became slower again (Fig. 1C). This temporary slowing in τ_{dw} resulted in >30% increase of the weighted decay time constant compared with P6-8 (mean τ_{dw} at P9-11: 126.1 ± 4.8 ms, $n = 25$; $P < 0.01$; Fig. 1F). At P12-16 (Fig. 1D), decay times were significantly faster compared with P3-5 and P9-11 and similar to durations in P17 mice or older (mean τ_{dw} at P12-16: 83.4 ± 9.1 ms, $n = 13$, and at P17-20: 76.8 ± 4.1 ms, $n = 8$; $P < 0.001$; Fig. 1D). We next analyzed the distribution of τ_{dw} for each age group (Fig. 1E). Decay constants were calculated from a minimum of 110 well-resolved individual sIPSCs recorded from 5-6 cells per age group, and the histogram was fitted with the best single Gaussian distribution. Data are plotted on a log ordinate with square root abscissa to facilitate display of distributions with both brief and long-lasting events (Sigworth and Sine 1987). Figure 1E illustrates that although decay constants were generally overlapping in their distributions at all age groups, the relative contribution of slow events, especially those outside of the Gaussian distribution, was greatest at P3-5 and P9-11. The peaks in each distribution show a clear progressive leftward shift with each stage of development, with the exception of P9-11, where there appears to be a pause, or even a transient reversal of the trend. Note that at the three earliest developmental stages, the IPSC τ_{dw} distributions

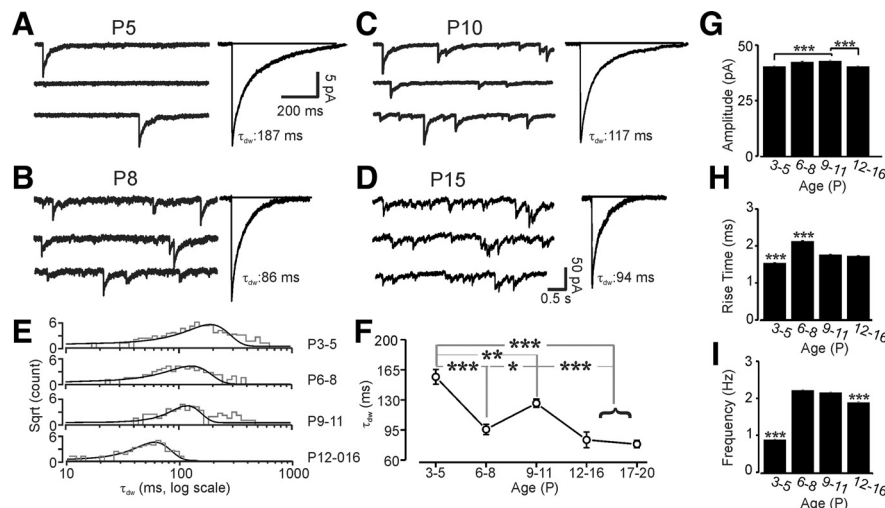


Fig. 1. Whole cell patch-clamp recordings of GABA-mediated spontaneous inhibitory postsynaptic currents (IPSCs) in thalamic reticular nucleus (nRt) neurons during development. Sample traces illustrate characteristic properties for each developmental stage. *A*: an example nRt cell at postnatal day 5 (P5) with slow monophasic events (*left*). Composite averaged sIPSC from this neuron (*right*) is shown on an expanded time scale to illustrate the long duration of response (weighted decay time constant $\tau_{dw} = 187$ ms). *B*: at P8, events were more frequent and faster ($\tau_{dw} = 86$ ms). *C*: at P10, sIPSC decay time was slower compared with that at P8 ($\tau_{dw} = 117$ ms). *D*: at P15, sIPSC decay durations became faster again as illustrated by the averaged IPSC ($\tau_{dw} = 94$ ms). *E*: histograms depicting sIPSC decay time distributions for each developmental stage. Data are derived from a minimum of 5 cells per age group ($n \geq 110$ events per age group). *F*: population data summarizing the bimodal time course of τ_{dw} during maturation. In *G*, the peak amplitude increased gradually, but significantly, from P3-5 to P9-11 and became significantly smaller later on (P12-16). For simplification, only statistical significance of $P < 0.001$ is shown in *G*. In *H*, fastest rise times (calculated as time required to rise from 10 to 90% of peak current amplitude) were observed at P3-5. Although rise times showed significant slowing at P6-8, they became faster again at P9-11 and beyond. *I*: sIPSC frequencies were significantly lower at P3-5 compared with all other age groups. Whereas sIPSC frequency dramatically increased at P6-8 and P9-11, sIPSC rates dropped significantly at P12-16. Values are means ± SE; for P3-5: $n = 28$, P6-8: $n = 13$, P9-11: $n = 25$, P12-16: $n = 13$, P17-20: $n = 8$. * $P < 0.05$; ** $P < 0.01$; *** $P < 0.001$; 1-way ANOVA was used to test for differences among the age groups. Tukey's post hoc comparisons indicate which of the group means were significantly different compared with every other group mean.

were poorly fit by single Gaussian distributions, with several bins in each case at the large end of the distribution (>100 ms) outside of the fitted Gaussian curve. Thus the peak for these curves is left-shifted (smaller) compared with the overall mean. The developmental pattern of change in sIPSC decay time follows a bimodal function with two distinct peaks at P3-5 and P9-11 (Fig. 1*F*). nRt neurons at these young ages also displayed developmentally dependent differences in peak current amplitude, rise time, and frequency (Fig. 1, *G-I*). Interestingly, the maturation pattern for these parameters followed a bidirectional time course similar to that already shown for the decay time constant. For example, sIPSC peak current amplitudes were significantly larger between P6-8 (42.8 ± 0.4 pA; $P < 0.01$) and P9-11 (43.2 ± 0.3 pA; $P < 0.001$) compared with recordings from cells at P3-5 (40.8 ± 0.3 pA) and P12-16 (40.9 ± 0.3 pA). Furthermore, sIPSC rise times, calculated as the time required to rise from 10 to 90% of peak current amplitude, were significantly slower at P6-8 (2.12 ± 0.02 ms; $P < 0.001$) compared with P3-5, when they were fastest (1.52 ± 0.01 ms; $P < 0.001$), and with P9-11 (1.75 ± 0.01 ms) and P12-16 (1.72 ± 0.01 ms). Finally, although sIPSCs occurred at very low frequencies in neonatal neurons (P3-5: 0.89 ± 0.02 Hz; $P < 0.001$), there was a substantial increase (over 100%) in frequency within 2 days (P6-8: 2.23 ± 0.02 Hz). These rates were sustained until P9-11 (2.17 ± 0.02 Hz), when we observed a significant decrease (P12-16: 1.9 ± 0.02 Hz; $P < 0.001$) again ($n = 15$ cells per age group).

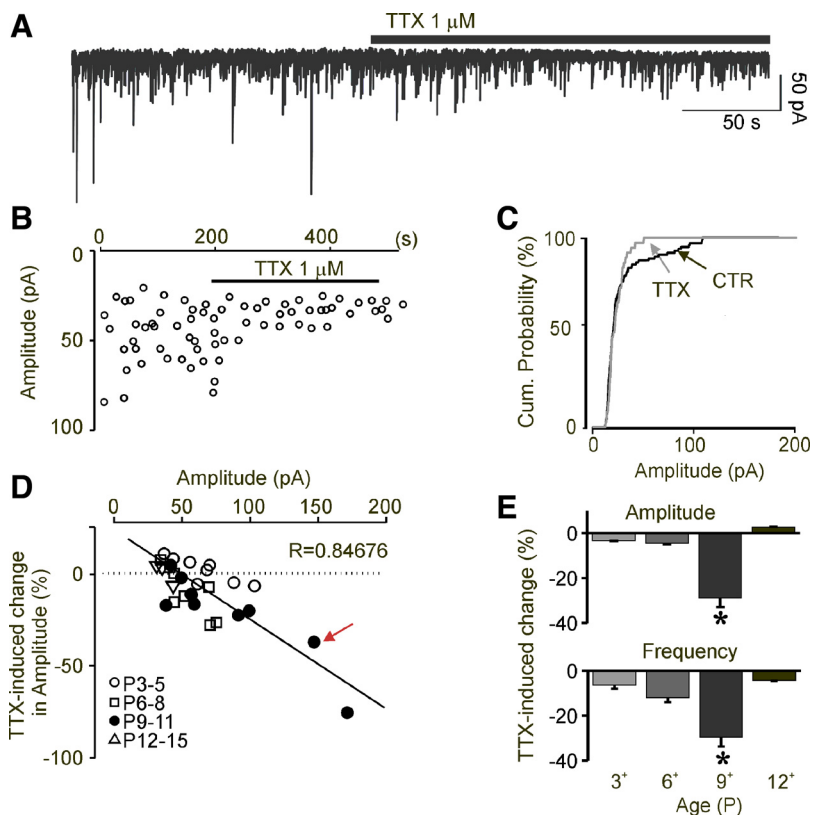
In summary, although sIPSC kinetics progressively became more adultlike during the developmental time period that we studied, there appears to be a short period at the beginning of the second postnatal week when inhibitory events were longer

in duration, had larger amplitudes and slower rise times, and occurred at higher frequencies.

Developmental changes in activity dependence of sIPSCs in nRt. Several mechanisms may account for these developmental changes in sIPSC kinetic properties, including pre- and post-synaptic changes (see DISCUSSION). One measure of presynaptic alterations is provided by TTX sensitivity, which can be used to probe the contribution of action potential-mediated synaptic responses to overall spontaneous events that also include action potential-independent synaptic response [miniature IPSCs (mIPSCs, or minis)]. Figure 2 shows the effect of TTX ($1 \mu\text{M}$) on sIPSCs at distinct developmental stages. An example of a recording from a P9 nRt cell (Fig. 2*A*) demonstrates that TTX blocked large-amplitude (>50 pA) sIPSCs (Fig. 2*B*). Thus the cumulative probability for sIPSCs was shifted to the left, especially for the upper quartile (Fig. 2*C*), suggesting that the majority of activity-dependent events were larger than ~ 50 pA. The sensitivity to TTX was correlated with the mean sIPSC peak amplitude. In Fig. 2*D*, the solid line represents the results of linear regression ($R = 0.85$, $P < 0.001$) between the TTX-induced reduction in sIPSC amplitude and control (i.e., pre-TTX) amplitude. Furthermore, TTX sensitivity is also associated with age, because only sIPSCs at P9-11 were found to be affected by TTX (mean reduction in amplitude = $32.5 \pm 4.4\%$ and in that frequency = $30.7 \pm 5.6\%$; $P < 0.05$; Fig. 2*E*). It is important to note that sIPSCs at this developmental stage had significantly larger peak current amplitudes, as described in Fig. 1*G*. The lack of TTX efficacy in other age groups suggests that at these developmental stages, the vast majority of sIPSCs are minis, i.e., those independent on action potential generation and therefore generated through spontaneous vesicle release events.

Fig. 2. Large sIPSCs at P9-11 are tetrodotoxin (TTX) sensitive.

A: sample trace obtained at P9 shows reduction in amplitude and frequency of sIPSCs in presence of TTX ($1 \mu\text{M}$). *B:* scatter plot of the same neuron illustrates sensitivity of large events to TTX blockade. Each point is the average amplitude of all sIPSCs within a given 3-s epoch. In the same cell, in *C*, the cumulative distribution of IPSC amplitudes demonstrates a reduction in the large-amplitude events after exposure to TTX, without changes in contribution of smaller (<20 pA) events. Pooled data in *D* demonstrate that the degree of TTX blockade is dependent on mean sIPSC amplitude. The solid line indicates the results of linear regression ($R = 0.85$, $P < 0.001$) between TTX effect and peak amplitude, suggesting that mainly currents >50 pA are blocked. Note that the largest TTX-dependent reduction in sIPSC amplitude occurred in two P9-11 neurons (filled circles) in which control (CTR) sIPSC amplitude was >100 pA. Red arrow marks the cell displayed in *A*, *B*, and *C*. *E:* age dependence of TTX sensitivity with significant reductions in amplitude ($32.5 \pm 4.4\%$; $P < 0.05$) and frequency ($30.7 \pm 5.6\%$; $P < 0.05$) only at P9-11. Values are means \pm SE; for P3-5: $n = 7$; P6-8: $n = 9$; P9-11: $n = 7$; P12-15: $n = 5$. * $P < 0.05$; paired Student's *t*-test.



Developmental postsynaptic changes in IPSCs in nRt cells. As described earlier, the kinetic properties of IPSCs are strongly influenced by the α -subunit isoform in the underlying GABA_AR. Therefore, we hypothesized that if these changes in IPSC morphology were caused by a developmental change of the α -subunit, this process should be reflected by altered sensitivity to α -subunit-specific benzodiazepine (BZ) modulators. In our first set of experiments, we tested for the contribution of the α_3 -subunit in immature nRt cells by using mice with an α_3 (H126R) point mutation (Low et al. 2000) that selectively renders GABA_ARs containing the α_3 -subunit insensitive to BZs but with otherwise normal function.

Clonazepam strongly enhances immature sIPSCs. In these experiments, we recorded sIPSCs from immature nRt neurons in α_3 (H126R) mice and their WT controls under control conditions and in the presence of CZP (100 nM). If BZ site-sensitive α -subunits other than α_3 contribute to synaptic GABA_AR function, the application of CZP would be expected to enhance sIPSCs in nRt cells from α_3 mutant mice. However, if the response to CZP in the WT is mediated mainly by α_3 -containing GABA_ARs, a reduced enhancement of sIPSCs in the α_3 mutant mice compared with WT controls would be anticipated. Based on a previous study that demonstrated transient perinatal expression of α_5 nRt (Studer et al. 2006) and our observation of slower sIPSC kinetics in neonatal nRt cells, we used an α_5 -specific site ligand to test for the presence of GABA_ARs containing the α_5 -subunit (Pearce 1993; Zarnowska et al. 2009).

We performed sequential recordings, first in control conditions, then in the presence of CZP, and finally during coapplication of CZP with the α_5 -subunit-selective inverse agonist L-655,708 (L-655; 15 nM), which antagonizes BZ effects. Figure 3 shows examples of the CZP-induced slowing of sIPSCs and the partial reversibility of this effect during L-655 application in immature nRt neurons, but not in cells older than P10. At P5, CZP prolonged sIPSCs not only in WT but also in α_3 (H126R) neurons (Fig. 3, A and B). In contrast, recordings at P15 (Fig. 3, C and D) showed reduced (WT) or abolished [α_3 (H126R)] sensitivity to CZP. The CZP-induced effect on decay time could be partially reversed by coapplication of L-655 in both genotypes at P5, but not at P15 (Fig. 3, A–D). These drug-induced changes in τ_{dw} and amplitude are presented in multiple comparison plots in Fig. 3, E1 and F1, respectively. They demonstrate the effect on individual nRt cells in WT and α_3 mutant mice for two developmental stages (each set of 3 symbols connected by 2 lines represents an individual cell). Figure 3, E2 and F2, shows the normalized population data for both age groups and genotypes: the effect of CZP on τ_{dw} (Fig. 3E2) was significantly stronger in P4–8 neurons of WT compared with α_3 mutant mice [mean increase in WT τ_{dw} : $84.5 \pm 21.8\%$, $n = 6$; $P < 0.05$; and in α_3 (H126R): $38.4 \pm 6.2\%$, $n = 14$; $P < 0.01$]. For P11–16, CZP elicited a significant increase in τ_{dw} in WT but not in α_3 mutant mice [WT: $35.3 \pm 4.5\%$, $n = 11$; $P < 0.01$; and α_3 (H126R): $6.8 \pm 2.2\%$, $n = 10$]. Coapplication of L-655 with CZP reversed the increase in decay time in P4–8 animals; however, this reversal was only statistically significant in α_3 mutant mice [mean effect on τ_{dw} in presence of CZP and L-655 compared with control values in WT: $49.3 \pm 14.6\%$, $n = 4$, and in α_3 (H126R): $21.5 \pm 5.9\%$, $n = 6$; $P < 0.05$]. At P11–16, coapplication of L-655 with CZP was without any effect in either genotype. We

also observed significant effects of CZP on IPSC amplitudes (Fig. 3F2). In general, there were more pronounced increases in the amplitude of sIPSCs at P4–8 [mean increase in WT: $30.7 \pm 8.1\%$, $n = 6$; $P < 0.01$; and in α_3 (H126R): $18.5 \pm 4.0\%$, $n = 14$; $P < 0.01$] than at P11–16 [mean increase in WT $12.8 \pm 3.6\%$, $n = 11$; $P < 0.05$; and in α_3 (H126R): $4.3 \pm 3.5\%$, $n = 10$]. Figure 3F2 also shows that L-655 had a significantly greater effect on the amplitude of α_3 mutant sIPSCs compared with WT [mean effect on amplitude in presence of CZP and L-655 compared with control values in WT: $19.6 \pm 4.3\%$, $n = 4$; $P < 0.05$; and in α_3 (H126R): $-11.8 \pm 3.1\%$, $n = 6$; $P < 0.05$]. At P4–8, coapplication of L-655 produced a larger reduction in sIPSC amplitude compared with the effect on decay time, but this effect was not observed in older mice. In conclusion, we found that CZP potentiates α_3 mutant sIPSCs at P4–8 but not at P11–16, indicating the presence of an α -subunit distinct from α_3 . In addition, the CZP-induced increase was significantly stronger in WT compared with α_3 (H126R) mice, which suggests that α_3 -subunits are already expressed, i.e., the expression of both GABA_AR α -subtypes overlaps. Finally, L-655 had a noticeable effect only on immature IPSCs. This suggests that GABA_ARs contain the α_5 -subunit only in developing nRt neurons.

α_3 (H126R) GABA_ARs are insensitive to zolpidem. Previous studies demonstrated that CZP potentiates not only GABA_ARs containing α_3 - and α_5 -subunits but also those containing α_1 - or α_2 -subunits (Dunning et al. 1999; Macdonald and Olsen 1994; Rudolph and Mohler 2004; Pritchett and Seeburg 1990). Because CZP dramatically enhanced GABA_ARs in immature nRt cells, we wanted to determine whether immature GABA_ARs also express the α_1 -isoform. The imidazopyridine zolpidem (ZLP) is a BZ ligand with high selectivity for receptors containing the α_1 -subunit and moderate affinity to α_2 - or α_3 -subunit, but with no sensitivity to α_5 -containing GABA_ARs (Maric et al. 1999). The rationale behind this approach is that if ZLP significantly enhanced sIPSCs at P4–8, the underlying GABA_AR combination should contain the α_1 -subunit, or potentially the α_2 - or α_3 -subunit. However, if sIPSC properties remained unchanged under ZLP application, then the presence of GABA_ARs containing α -subunits that are insensitive to ZLP, such as the α_5 -subunit, would be indicated. Figure 4 shows recordings of two age groups of nRt cells from WT and α_3 (H126R) slices in control conditions and in the presence of ZLP. For recordings from P5 neurons, ZLP showed only a minor, nonsignificant effect on sIPSC from WT (Fig. 4A) and had no noticeable effect in α_3 mutant mice (Fig. 4B). In contrast, ZLP increased averaged sIPSCs at P15 in neurons of WT (Fig. 4C) but not α_3 (H126R) mice (Fig. 4D). The effects of ZLP on sIPSC τ_{dw} and amplitude from individual recordings in WT and α_3 mutant mice are illustrated in Fig. 4, E1 and F1, respectively. Finally, Fig. 4, E2 and F2, summarizes how ZLP sensitivity changed during development. We found that at P4–8, sIPSC τ_{dw} was not significantly affected in WT ($6.5 \pm 4.2\%$, $n = 4$). ZLP sensitivity increased during development in WT GABA_ARs such that at P11–16, ZLP increased sIPSC τ_{dw} by $35.3 \pm 3.2\%$ ($n = 6$; $P < 0.01$). In contrast, there was no developmental change in ZLP sensitivity in mice carrying the BZ-insensitive GABA_AR α_3 -subunit; at all ages the sIPSCs remained ZLP insensitive. These results further support the conclusion that GABA_ARs in immature (P4–8) neurons express α_5 -subunits.

Early expression of α_5 GABA_AR subtype. On the basis of our previous observations, we suggest that differences in the kinetic properties of inhibitory synaptic currents result from changes in the underlying molecular structure of the GABA_AR. We used immunohistochemistry to confirm that α_5 -subunits are transiently expressed in immature nRt cells and to determine whether there might be a developmental period in which they are coexpressed with the α_3 -subunit. Figure 5 shows the distribution of GABA_AR subtypes in horizontal sections of thalamic slices at P5 (*left*) and at P20 (*right*). These slices have been processed with subunit-specific antibodies for GABA_AR subunits α_1 (Fig. 5A), α_3 (Fig. 5B), and α_5 (Fig. 5C). For α_1 -subunit-containing GABA_ARs, we did not observe antibody staining in nRt cells at P5 (Fig. 5A1) or P20 (Fig. 5A2). However, intense immunoreactivity (IR) could be detected in the globus pallidus and slightly less in caudate putamen at both

ages. As also shown in Fig. 5A1, only weak labeling for α_1 -subunit IR could be seen in the ventrobasal complex (VB) in slices at P5, in contrast to a robust expression at P20 (Fig. 5A2). Note that this delayed expression of α_1 (preceded by α_2) IR in VB has been described in earlier studies (Peden et al. 2008). The α_3 -subunit showed strong nRt staining at P5 and persistence at a somewhat lower level at P20 (Fig. 5B). We found prominent staining for α_5 only during early development (Fig. 5C1). Staining for α_5 IR was no longer present in nRt at P20 (Fig. 5C2). The above results highlight developmental changes in nRt GABA_AR subunit immunoreactivity that correspond to the functional changes in synaptic inhibition. Although it is possible that knockin of BZ insensitivity to the α_3 GABA_AR subunit might result in a different developmental profile, the initial characterization of these mice indicated that overall GABA_A receptor expression was not disrupted (Low et al. 2000).

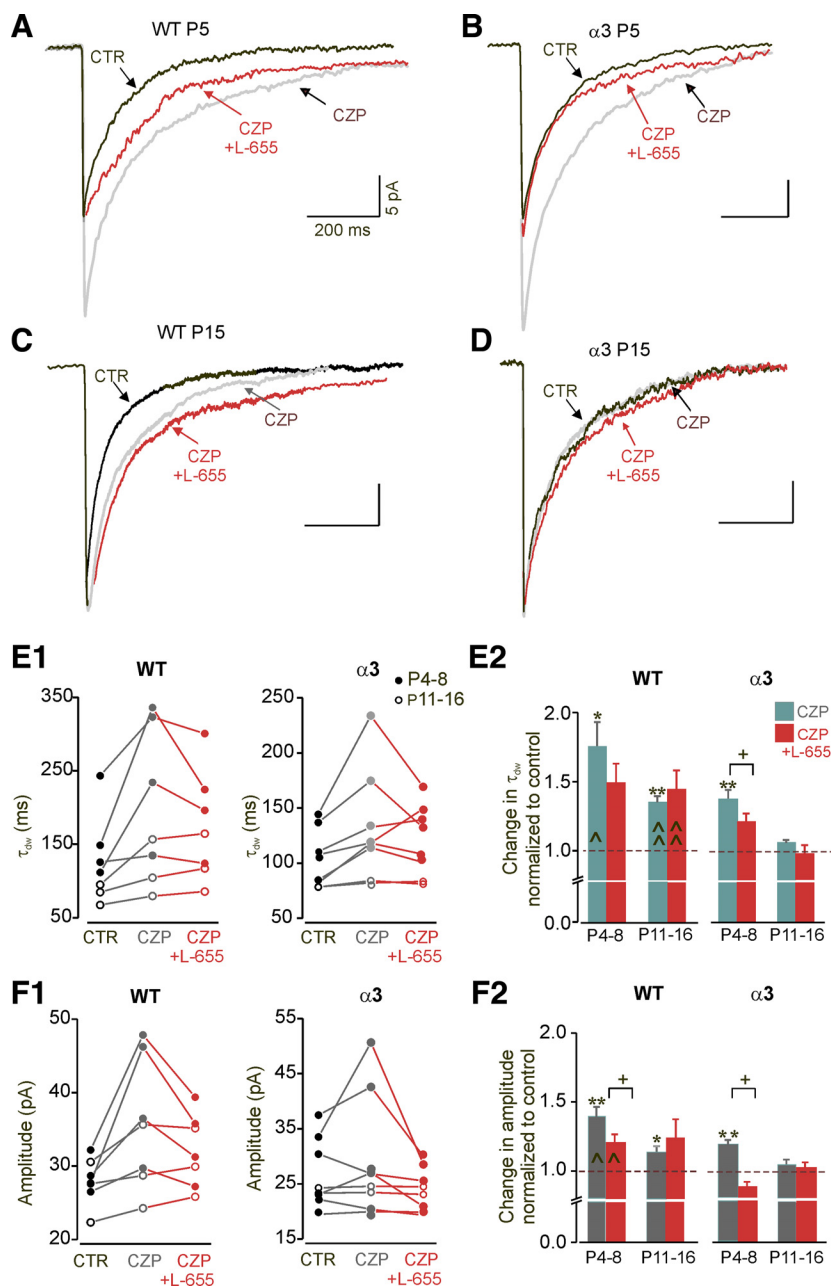


Fig. 3. Immature synaptic GABA_A receptors (GABA_ARs) are highly benzodiazepine (BZ) sensitive and not strictly dependent on α_3 -subunits. Properties of sIPSCs at different age groups in CTR, 100 nM clonazepam (CZP) and 100 nM CZP + 20 nM L-655,708 (L-655). *A* and *B*: averaged sIPSCs from P5 wild-type (WT) and α_3 (H126R) mutant (α_3) mice, respectively, show strong CZP-dependent increase together with significant L-655-dependent reduction in sIPSC amplitude and decay time. *C* and *D*: CZP efficacy at P15 in WT but not α_3 (H126R); L-655 was ineffective in both genotypes at this age. *E* and *F*: CZP-induced increase and partial L-655-dependent reduction of sIPSC τ_{dew} (*E1*) and amplitude (*F1*) in individual WT and α_3 (H126R) cells at P4-8 (filled circles) but not at P11-16 (open circles), when CZP efficacy was weaker in WT and absent in α_3 neurons. *E2* shows normalized responses indicating a decrease in CZP efficacy for WT and α_3 (H126R) sIPSC τ_{dew} from P4-8 to P11-16. CZP efficacy increased at both age groups in WT but only at P4-8 in α_3 (H126R). *F2* shows an average increase of 30.7% ($n = 6$) in WT amplitude at P4-8 and significantly less increase of 18.5% ($n = 10$) in α_3 (H126R). At P4-8, WT sIPSC amplitude was decreased to less than control by L-655. There was a 12.8% CZP-dependent increase in WT amplitude at P11-16 but no effect in α_3 (H126R) cells. No effect of L-655 on amplitude was found at this developmental stage. Statistical significance: * $P < 0.05$; ** $P < 0.01$, CZP compared with control. + $P < 0.05$; ++ $P < 0.01$, L-655 compared with CZP. ^ $P < 0.05$; ^^ $P < 0.01$, WT compared with α_3 (H126R); Student's *t*-test.

The α_5 -subunit-containing GABA_AR has been identified at extrasynaptic locations in hippocampus (Caraiscos et al. 2004; Crestani et al. 2002). To differentiate between synaptic and extrasynaptic location of immature GABA_ARs, we used confocal microscopy for either α_3 - or α_5 -subunit IR double-stained with the scaffold protein gephyrin, which is implicated in the synaptic localization of GABA_ARs (Luscher and Keller 2004; Yu et al. 2007). α_3 IR and gephyrin costaining was quite rare at P5, whereas at P30 multiple clusters could be observed near presumed cell bodies (Fig. 6, *A1* and *A2*, arrows). This finding indicates that the extent of synaptic α_3 -containing GABA_ARs increases during development. In contrast, colocalization of α_5 with gephyrin was sparse but present at P5, but largely absent at P30 (Fig. 6, *B1* and *B2*). The small number of gephyrin clusters colocalized with either α_3 - or α_5 -subunit IR during the first postnatal week suggests that many GABA_ARs are not associated with synaptic locations at this stage.

Tonic currents mediated by immature GABA_ARs have distinct pharmacology. Because varying combinations of GABA_ARs containing α_5 subtypes have been shown to mediate tonic currents (Mohler 2006; Semyanov et al. 2004), we tested whether tonic GABA_AR activation mediated by α_5 -subunits plays a role in the nRt. Tonic GABA_AR activation could be developmentally regulated similar to other brain regions (LoTurco et al. 1995; Nusser and Mody 2002; Stell and Mody 2002), such as in immature hippocampal pyramidal neurons, where a significant tonic current can only be detected during early development (Demarque et al. 2002). Therefore, we tested the response of bath-applied GABA (5–10 μ M) and the GABA_AR antagonist gabazine (GBZ; 0.2 and 10 μ M) on currents recorded at two stages of development, perinatal (P5) and mature (P24–30; Fig. 7). Figure 7*A* shows that 5 μ M GABA induced an inward shift in the baseline holding current

(I_{hold}) at both ages, but with a much larger inward shift at P5 (*top*) compared with P24 (*bottom*). This GABA-induced shift in I_{hold} could be reversed by subsequent GBZ application, and post-GBZ levels were more positive than baseline, especially in P5 cells, indicating that some tonic GABA_A conductance was active even in the absence of exogenous GABA. The shifts in I_{hold} were accompanied by changes in background noise (I_{SD}), as illustrated in Fig. 7*C*. These differences in background noise are correlated with magnitude of active tonic GABA conductance and correspond in part to the modulation of stochastic channel openings resulting from the activation and inhibition of tonically active GABA_ARs by GABA and GBZ, respectively (Brickley et al. 1996; Kaneda et al. 1995; Wall and Usowicz 1997). Analysis of the cells from Fig. 7*A* revealed that bath-applied GABA caused an inward shift in I_{hold} as well as an increase in background noise of currents at P5 (Fig. 7*B*, *top*), whereas it had less effect at P24 (Fig. 7*B*, *bottom*). Coapplication of low-dose GBZ (0.2 μ M) decreased the GABA-induced background noise at P5, but not at P20–26. We estimated I_{SD} from Gaussian fits of all-point-histograms based on the current amplitude [see MATERIALS AND METHODS (Sipila et al. 2007)]. The all-points histograms for the two representative neurons from Fig. 7*A* are shown in Fig. 7*B*. For Fig. 7*C*, we calculated the mean I_{SD} from Gaussian fits from all-points histograms under control, GABA, and low- and high-dose GBZ conditions. Results obtained by using I_{SD} as an imperfect estimate of tonic GABA_A receptor activation (it will be contaminated by other biological and instrument noise) suggest higher amplitudes of intrinsic GABA_AR tonic conductances for the older compared with younger age groups (mean I_{SD} in control at P5: 5.3 ± 0.6 pA and at P24–31: 6.5 ± 0.4 pA). In addition, we found higher GABA sensitivities in immature neurons such that at P5, GABA increased I_{SD} to 15.7 ± 1.7 pA.

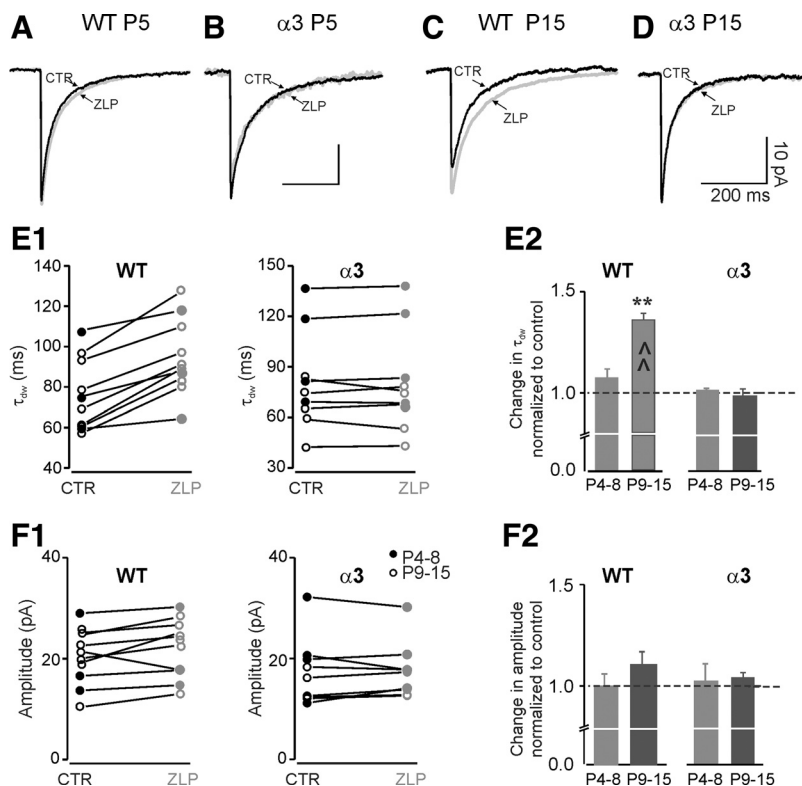


Fig. 4. Immature GABA_ARs are relatively insensitive to zolpidem (ZLP). Averaged sIPSCs of a representative P5 cell illustrate mild increase of decay time by ZLP (100 nM) in WT (*A*) but not α_3 (H126R) neurons (*B*). At P15, ZLP strongly slowed sIPSC decay in WT (*C*) but not in α_3 (H126R) (*D*). *E*: ZLP effects on sIPSC duration. In *E1*, individual cells from WT mice illustrate greater increases in τ_{dw} at P9–15 (open circles) compared with P4–8 (filled circles). In contrast, ZLP did not have any effect in α_3 (H126R) mice at any age. In *E2*, at P4–8, ZLP failed to increase sIPSC τ_{dw} in either WT ($6.5 \pm 4.2\%$, $n = 4$; not significant, NS) or α_3 (H126R) ($1.3 \pm 0.9\%$, $n = 4$, NS). In contrast, at P11–15, the mean increase in τ_{dw} was $35.3 \pm 3.2\%$ in WT ($n = 6$; $P < 0.01$), whereas there was no effect in the α_3 mutant ($n = 5$). The effect of ZLP on sIPSC τ_{dw} was significantly different between WT and α_3 (H126R) at P11–15 ($P < 0.01$), but not in younger mice. *F*: ZLP effects on sIPSC amplitude. In *F1*, there was insignificant increase in sIPSC amplitude at all ages in WT, but not for mutant cells. In *F2*, there was no significant effect on sIPSC amplitude in any age group or genotype. Statistical significance: * $P < 0.05$; ** $P < 0.01$, ZLP compared with control. $\wedge P < 0.05$; $\wedge\wedge P < 0.01$, WT compared with α_3 (H126R); Student's *t*-test.

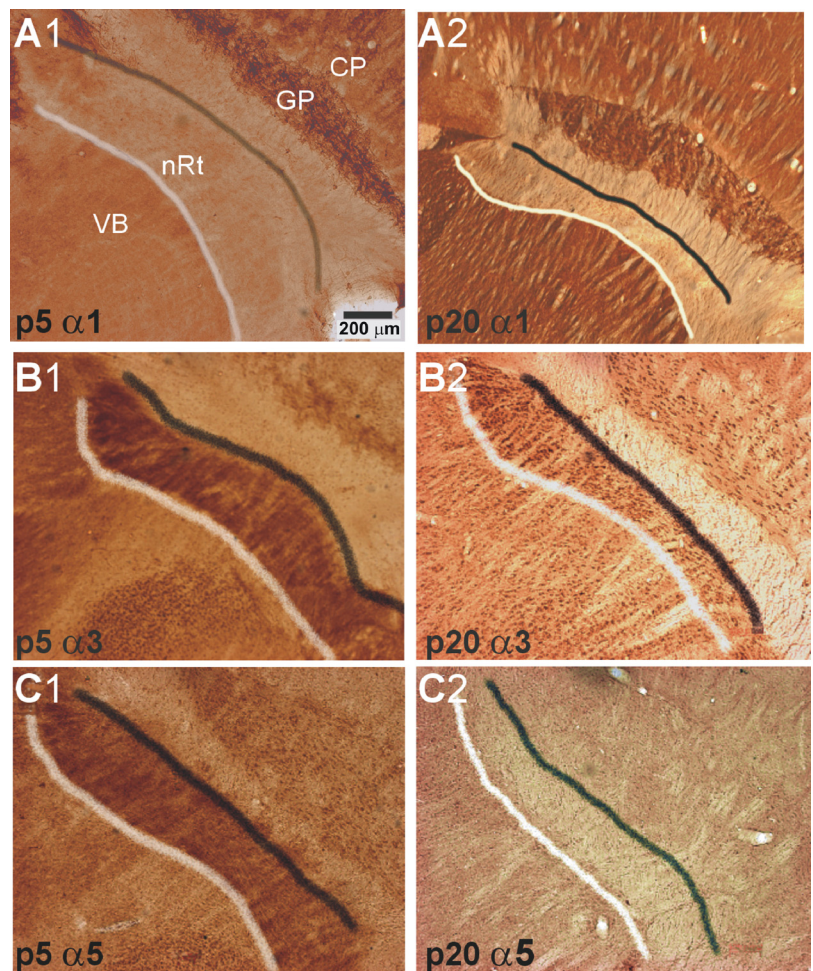


Fig. 5. Postnatal maturation of GABA_AR expression in the mouse thalamus shows coexpression of α_3 - and α_5 -subunits in nRt during early development. A–C: distribution of α_1 , α_3 , and α_5 immunoreactivity (IR) in horizontal sections of P5 and P20 slices processed for diaminobenzidine and subunit-specific antibodies. Borders outlining nRt are manually added for visibility. A1: weak α_1 IR could already be detected in ventrobasal complex (VB) at P5, which increased during development with prominent staining at P20 (A2). Also, strong immunolabeling for α_1 was present in globus pallidus (GP), with slightly less in caudate putamen (CP), at both ages. B1: intense α_3 IR was largely restricted to nRt, and whereas somata were relatively evenly labeled at P5, staining for neuronal processes was diffuse. B2: at P20, individual patches indicating mainly somatic labeling could clearly be identified, whereas processes remained unstained. C1: at P5, the diffuse staining of neuronal processes for α_5 IR was similar to that for α_3 IR at P5 (see B1), whereas the somatic labeling of α_5 IR resembled the patchy staining pattern observed for the α_3 -subunit at P20 (see B2). C2: α_5 IR was almost completely absent in nRt at P20. Scale bar, 200 μ m.

In contrast, there was significantly less enhancement in the older group (11 ± 0.8 pA). Interestingly, during coapplication with GBZ at low doses of 0.2 μ M, the GABA-enhanced I_{SD} was significantly reversed at P5 ($51 \pm 1.8\%$) but had only a weak effect at P24 ($26 \pm 3.2\%$; Fig. 7D; mean I_{SD} after 0.2 μ M GBZ at P5: 7.8 ± 1.5 pA; $P < 0.05$; and at P24–30: 8.2 ± 0.9 pA; $P < 0.05$). Furthermore, high-dose GBZ (10 μ M) application decreased I_{SD} to less than in control conditions and, as such, had a stronger effect in immature neurons ($86 \pm 1.4\%$) compared with the older age group ($74 \pm 3.6\%$; mean I_{SD} after 0.2 μ M GBZ at P5: 2.1 ± 0.2 pA; $P < 0.05$; and at P24–30: 2.7 ± 0.2 pA, $n = 6$ per age group).

We also calculated the shift in I_{hold} for each condition (GABA, low- and high-dose GBZ; not shown). There was a significantly larger shift of the GABA-enhanced I_{hold} at P5, increasing I_{hold} from 60.2 ± 7.3 to 167.4 ± 20.0 pA in cells of the younger age group compared with an increase in more mature neurons from 13.9 ± 6.6 to 47.9 ± 12.0 pA ($P < 0.001$). However, low concentrations of GBZ (0.2 μ M) reduced the GABA-enhanced I_{hold} to 66.6 ± 17.0 pA at P5, which is close to the level seen under control conditions, and at P24–30, we measured 25.5 ± 6.4 pA ($n = 6$; $P < 0.05$, independent Student's t -test). Our results suggest that tonic GABA_AR-mediated signaling occurs more robustly in immature and juvenile nRt neurons and that the degree of tonic GABA_AR activation (i.e., magnitude of tonic current) is age

dependent, presumably because of differences in the underlying α -subunit composition.

DISCUSSION

Previously, we described the presence of thalamic giant depolarizing potentials (tGDPs) in neonatal nRt neurons. These GABAergic events appear to play a role in circuit formation (Pangratz-Fuehrer et al. 2007). The present study examined how altered GABA_AR subunit compositions affect intrathalamic inhibition during early development. Briefly, we showed that 1) the GABA_AR α_5 -subunit is transiently expressed in nRt cells during the first two postnatal weeks, 2) the decline of α_5 expression is paralleled by a decrease of IPSC decay, 3) key electrophysiological properties of sIPSCs undergo a biphasic change; and 4) tonic GABA_AR-mediated conductance is stronger during the first postnatal week.

Does bidirectional change in IPSC kinetics reflect transient α_3/α_5 coexpression? One of the main findings of this study is the bimodal time course for IPSC decay time constants in nRt neurons between P3 and P18. Slowest IPSC decay times were observed at P3–5, becoming faster at P6–8. Surprisingly, at P9–11, we found a temporal slowing, followed by acceleration in cells older than P12. Multiple reasons could account for this bimodal time course. Given that the GABA_AR α_5 -subunit is transiently expressed in neonatal nRt neurons, as shown here and previously (Poulter et al. 1992; Studer et al. 2006), differ-

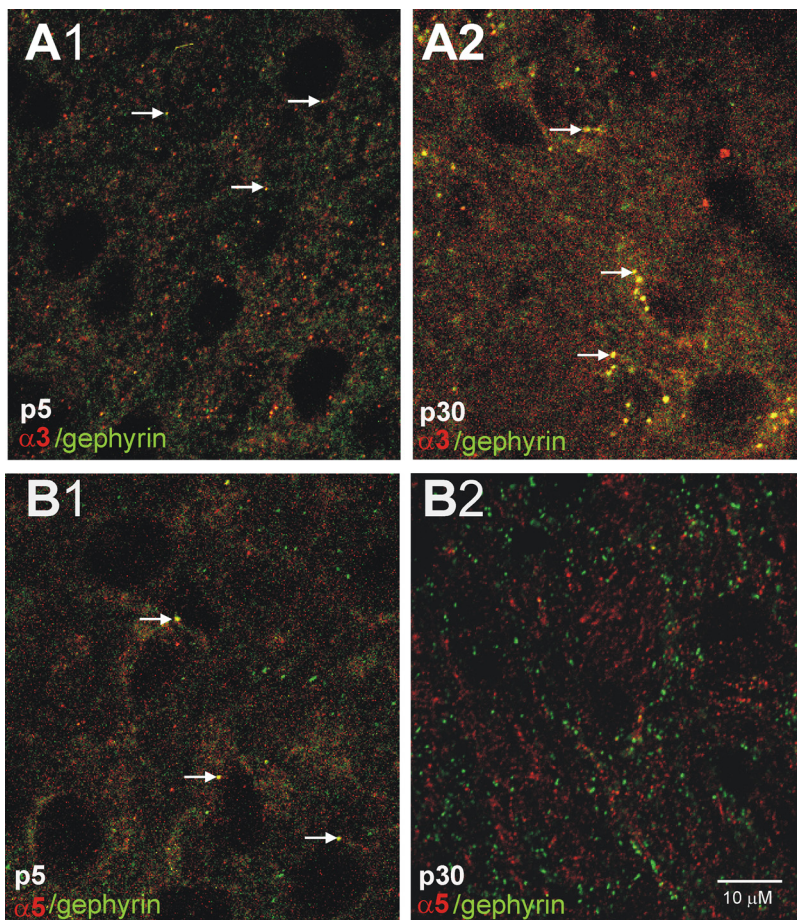


Fig. 6. Double immunofluorescence labeling of α_3 - and α_5 -subunits with gephyrin in nRt cells at P5 and P30. In *A*, confocal images show few colocalizations (arrow/yellow punctae) of gephyrin with α_3 at P5 (*A1*). In contrast, double staining of α_3 /gephyrin cluster is evident at P30 (*A2*), most prominently located surrounding the soma. Whereas *B1* illustrates a few colocalized α_5 /gephyrin punctae at P5 in somatic locations, these were absent at P30 (*B2*). Scale bar = 10 μm .

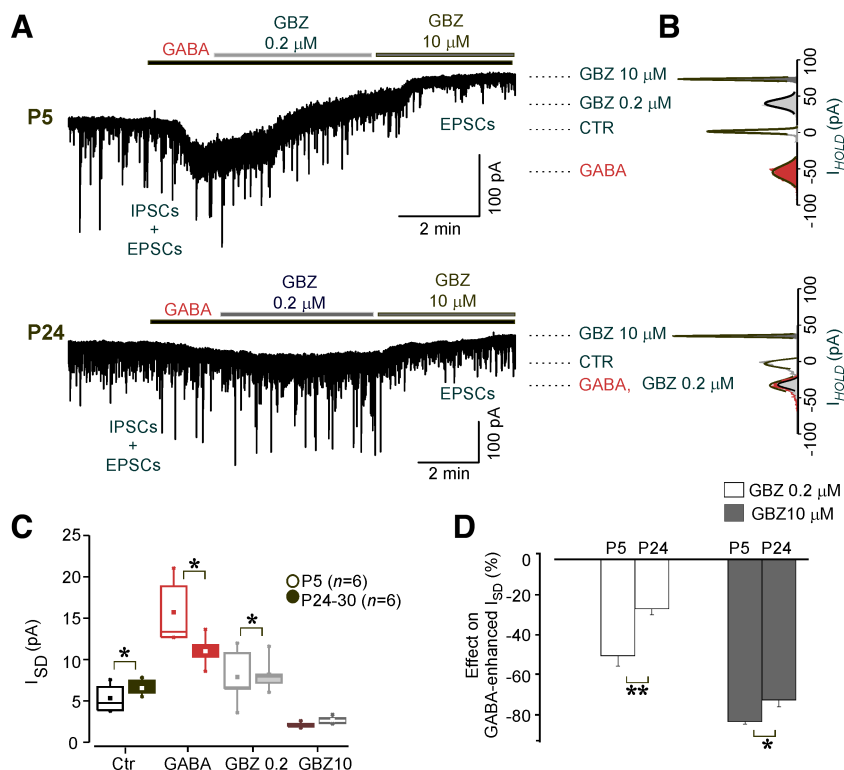
ences in decay time would be expected as a result of decreased expression of α_5 and replacement with other α -subunits. We tested this hypothesis with double staining for α_3 and α_5 at several developmental stages. Indeed, at P5 we found strong expression of α_5 with less prominent expression of α_3 , whereas this ratio had reversed at P11. Although there is precedent for progressive shortening of IPSC decay time during development due to subunit turnover (Dunning et al. 1999; Hollrigel and Soltesz 1997; Hutcheon et al. 2004; Okada et al. 2000; Vicini et al. 2001), this would not account for the transient slowing of sIPSCs at P9-11, which suggests another mechanism independent of GABA_AR subunit changes. Recently, it has been shown that editing of RNA transcripts encoding the α_3 -subunit undergoes developmental regulation (Rula et al. 2008). Editing activity peaked at P7; thus non-edited cells dominate during the first postnatal week. GABA_AR containing non-edited α_3 -subunits exhibit faster activation and slower deactivation times compared with edited receptors. The fact that we recorded sIPSCs with fastest rise and slowest decay times at P3-5 argues for a coexpression of non-edited α_3 -subtype together with GABA_AR containing α_5 . Faster sIPSC kinetics at P6-8 might correspond to increased numbers of edited α_3 GABA_AR accompanied by declining α_5 -subunits. ZLP, which is selective for α_1 and α_3 , but not α_5 , had no effect on sIPSC duration of neonatal nRt neurons (Fig. 4). CZP had significantly stronger effects in immature WT compared with mutant mice, indicating that α_3 already contributes to

functional inhibition at P3-5. The lack of significant ZLP effect at this stage, however, suggests that the contribution of α_3 is minor.

Effect of TTX is age dependent. A second key finding of this study was the apparent increase in activity-dependent inhibition at P6-8, which may contribute to the transient slow sIPSC kinetics and could explain why TTX blocked large sIPSCs exclusively at P9-11. Activity-dependent events may have different kinetic properties, as evidenced by the multimodal distribution of decay times at this age (Fig. 1E). This suggests that the activity-dependent release of GABA is capable of activating even extrasynaptic GABA_ARs (Herd et al. 2013; Rovo et al. 2014). A related developmental progression in nRt cell intrinsic excitability has been demonstrated (Warren and Jones 1997). The ability of nRt cells to produce low-threshold spikes (LTS) evoking multiple action potentials is age dependent. Bursting was only observed after P10-11 and could then induce network activation via triggering of rebound spikes in relay neurons. This suggests an activity-dependent maturation of nRt neurons, particularly during the first postnatal week, when a “critical period” was already determined for structural plasticity of developing thalamocortical synapses (Crair and Malenka 1995).

Tonic inhibition is more robust in immature nRt neurons. A tonic GABA_AR-mediated conductance was demonstrated in both immature and mature nRt neurons (Fig. 7). Tonic inhibition has been discovered in a variety of neuronal types (see review, Glykys and Mody 2007), including other thalamic

Fig. 7. Tonic GABA_AR current is more prominent in immature nRt neurons. *A, top*: sample trace at P5 shows strong activation of tonic current during bath application of 5 μ M GABA. Tonic current was reduced by 0.2 μ M GBZ and eliminated by 10 μ M GBZ. *Bottom*, in comparison, at P24, there is only weak activation of tonic GABA_AR and GBZ is subsequently less effective. *B*: an all-points histogram based on the steady holding current (I_{hold}) of the same neurons as in *A* illustrates high sensitivity of tonic current to GABA and GBZ at P5, but not at P24. In the latter, only little current was induced by GABA, and that which was produced was insensitive to low-dose GBZ. *C*: pooled data of Gaussian fits from all-points histograms of voltage-clamp I_{hold} show significant differences in background noise (I_{SD}) between age groups, which demonstrates that the degree of tonic GABA_AR activation (i.e., magnitude of tonic current) is age dependent. Furthermore, data in *D* illustrate that immature nRt neurons showed higher sensitivity to GBZ, suggesting that only high-dose GBZ can efficiently block tonic currents in mature nRt cells. Values are means \pm SE; $n = 6$ per age group. * $P < 0.05$; ** $P < 0.01$; *** $P < 0.001$; independent Student's *t*-test.



nuclei such as VB and lateral geniculate nucleus (Belelli et al. 2005; Bright et al. 2007; Cope et al. 2005; Peden et al. 2008; Wafford et al. 2009). However, these studies did not detect GABA-mediated tonic currents in nRt.

Various factors may explain this difference. First, much of the work examining tonic inhibition in the thalamus used adult animals. The fact that we observed the largest tonic current in immature nRt neurons does not diminish their relevance, because synaptic GABAergic activity is already present at this age. Nonetheless, we cannot exclude the possibility that inefficient GABA uptake might at least partially explain the prominent tonic current in early postnatal nRt cells. However, another study found that even in immature tissue, blocking GABA transporters enhanced the endogenous tonic current twofold in hippocampal pyramidal neurons (Sipila et al. 2007), suggesting that transporter function is already functional at this stage and that GABA transporters might play a significant role in extrasynaptic signaling.

Similarly, a significant reduction in tonic current has been described in developing cortical neurons. For newborn mice, the charge contributed by tonic current accounted to nearly 100% of the total GABA charge but decreased to 50% by the second postnatal week (Sebe et al. 2010). A second factor that could contribute to differences between our observations and previous studies is the higher concentration of GABA (10 μ M) used in our experiments, due to the fairly weak effect of 1 μ M GABA (not shown). Taken together, these findings suggest that, compared with adult cells, immature nRt neurons have a significantly higher reserve of GABA_AR-mediated tonic current. The fact that low GBZ concentrations (0.2 μ M) affected tonic current only in immature neurons suggests functional differences in the underlying GABA_AR in P5 compared with mature neurons. This selective sensitivity to low GBZ concentrations at P5 is inconsistent with decreased GABA uptake at

that developmental stage in that decreased uptake would increase GABA concentrations leading to less, not more, blockade by the competitive antagonist GBZ. Given that mature nRt neurons express scant synaptic α_5 (Figs. 5 and 6), it is unlikely that this subunit contributes to tonic conductance in the post-neonatal period. This offers the possibility that tonic currents are mediated by α_3 -containing GABA_AR (Devor et al. 2001) or, less likely, the δ -subunit (Peng et al. 2002; Porcello et al. 2003; Wisden et al. 1992) as shown for cells in VB (Belelli et al. 2005; Bright et al. 2007; Cope et al. 2005; Jia et al. 2005, 2008; Porcello et al. 2003), granule cells in dentate gyrus (Maguire et al. 2005; Nusser and Mody 2002), and cerebellum (Stell et al. 2003). CZP enhanced tonic currents in most nRt cells, but not all (not shown), indicating that these neurons can express various subtypes of GABA_AR at extrasynaptic locations responding differently to drugs, as observed in hippocampus (Glykys et al. 2008; Seymour et al. 2009).

Given that early in postnatal life, GABAergic transmission in nRt is excitatory (Pangratz-Fuehrer et al. 2007), we hypothesize that activation of the tonic current will depolarize the resting membrane potential of immature nRt neurons. The depolarizing influence on the intra-nRt network could act as major drive contributing to tGDP generation, thus creating a recurrent excitatory network within nRt, which would likely be amplified by the reciprocal connectivity with thalamocortical (TC) neurons. In the adult, a significant GABAergic tonic current would hyperpolarize nRt neurons and suppress the intra-nRt network via shunting inhibition. The reduced bursting activity of nRt neurons and the resultant attenuation of the inhibitory output received by TC neurons could explain the previously reported suppression of thalamic oscillations during pathological spike-wave discharges (Huguenard and Prince 1994; Huntsman et al. 1999; Sohal et al. 2000; von Krosigk et al. 1993). In the developing hippocampus, tonic inhibition can

block the generation of synaptic GABAergic inhibition (Grantyn et al. 2011), whereas a complete lack results in spontaneous gamma oscillations in vitro (Glykys et al. 2008).

Dysfunctional extrasynaptic inhibition can produce an epileptic phenotype (Zhu et al. 2011). In the thalamus, blockade of intra-nRt inhibition facilitates epileptiform discharge (Sohal and Huguenard 2003). Interestingly, the complete loss of the α_3 -subunit protein in the nRt (α_3 knockout mouse) did not result in an overtly different behavioral phenotype but displayed retention of nRt GABA_A receptor signaling, suggesting that other α -subunits may compensate for the loss of α_3 (Schofield and Huguenard 2007).

Conclusion. Together, these results suggest that the early expression of α_5 -subunits in nRt cells prolongs the duration of synaptic inhibitory responses. This slow mode of inhibition could be required for early circuit development. Specifically, because GABA is considered a promoter for maturation and synaptogenesis, slower transmission could enhance this function. Furthermore, α_5 -containing GABA_ARs could mediate the early postnatal tonic current. Biphasic changes in GABAergic transmission could reflect the induction of network activation, with the developmental shortening of IPSCs promoting faster rhythmic oscillations at a time when fast signal transduction and higher levels of consciousness are required after the enhanced awareness of the external environment, i.e., the time of eye opening.

GRANTS

This work was supported by National Institute of Neurological Disorders and Stroke Grants NS06477 and NS34774 and by Austrian Science Fund Project J2222-B04.

DISCLOSURES

No conflicts of interest, financial or otherwise, are declared by the authors.

AUTHOR CONTRIBUTIONS

S.P.-F. and J.R.H. conception and design of research; S.P.-F. performed experiments; S.P.-F., I.P., and J.R.H. analyzed data; S.P.-F., W.S., U.R., I.P., and J.R.H. interpreted results of experiments; S.P.-F. prepared figures; S.P.-F. drafted manuscript; S.P.-F., W.S., U.R., I.P., and J.R.H. edited and revised manuscript; S.P.-F., W.S., U.R., I.P., and J.R.H. approved final version of manuscript.

REFERENCES

- Avanzini G, Vergnes M, Spreafico R, Marescaux C. Calcium-dependent regulation of genetically determined spike and waves by the reticular thalamic nucleus of rats. *Epilepsia* 34: 1–7, 1993.
- Belelli D, Peden DR, Rosahl TW, Wafford KA, Lambert JJ. Extrasynaptic GABA_A receptors of thalamocortical neurons: a molecular target for hypnotics. *J Neurosci* 25: 11513–11520, 2005.
- Brickley SG, Cull-Candy SG, Farrant M. Development of a tonic form of synaptic inhibition in rat cerebellar granule cells resulting from persistent activation of GABA_A receptors. *J Physiol* 497: 753–759, 1996.
- Bright DP, Aller MI, Brickley SG. Synaptic release generates a tonic GABA_A receptor-mediated conductance that modulates burst precision in thalamic relay neurons. *J Neurosci* 27: 2560–2569, 2007.
- Brooks-Kayal AR. Rearranging receptors. *Epilepsia* 46, Suppl 7: 29–38, 2005.
- Brooks-Kayal AR, Shumate MD, Jin H, Rikhter TY, Coulter DA. Selective changes in single cell GABA_A receptor subunit expression and function in temporal lobe epilepsy. *Nat Med* 4: 1166–1172, 1998.
- Caraballo RH, Dalla BB. Idiopathic generalized epilepsies. *Handb Clin Neurol* 111: 579–589, 2013.
- Caraiscos VB, Elliott EM, You T, Cheng VY, Belelli D, Newell JG, Jackson MF, Lambert JJ, Rosahl TW, Wafford KA, MacDonald JF, Orser BA. Tonic inhibition in mouse hippocampal CA1 pyramidal neurons is mediated by α_5 subunit-containing γ -aminobutyric acid type A receptors. *Proc Natl Acad Sci USA* 101: 3662–3667, 2004.
- Cherubini E, Conti F. Generating diversity at GABAergic synapses. *Trends Neurosci* 24: 155–162, 2001.
- Christian CA, Herbert AG, Holt RL, Peng K, Sherwood KD, Pangratz-Fuehrer S, Rudolph U, Huguenard JR. Endogenous positive allosteric modulation of GABA_A receptors by diazepam binding inhibitor. *Neuron* 78: 1063–1074, 2013.
- Cope DW, Hughes SW, Crunelli V. GABA_A receptor-mediated tonic inhibition in thalamic neurons. *J Neurosci* 25: 11553–11563, 2005.
- Cossette P, Liu L, Brisebois K, Dong H, Lortie A, Vanasse M, Saint-Hilaire JM, Carmant L, Verner A, Lu WY, Wang YT, Rouleau GA. Mutation of GABRA1 in an autosomal dominant form of juvenile myoclonic epilepsy. *Nat Genet* 31: 184–189, 2002.
- Crair MC, Malenka RC. A critical period for long-term potentiation at thalamocortical synapses. *Nature* 375: 325–328, 1995.
- Crestani F, Keist R, Fritschy JM, Benke D, Vogt K, Prut L, Bluthmann H, Mohler H, Rudolph U. Trace fear conditioning involves hippocampal α_5 GABA_A receptors. *Proc Natl Acad Sci USA* 99: 8980–8985, 2002.
- DeLorey TM, Handforth A, Anagnostaras SG, Homanics GE, Minassian BA, Asatourian A, Fanselow MS, Delgado-Escueta A, Ellison GD, Olsen RW. Mice lacking the β_3 subunit of the GABA_A receptor have the epilepsy phenotype and many of the behavioral characteristics of Angelman syndrome. *J Neurosci* 18: 8505–8514, 1998.
- Demarque M, Represa A, Becq H, Khalilov I, Ben Ari Y, Aniksztejn L. Paracrine intercellular communication by a Ca²⁺- and SNARE-independent release of GABA and glutamate prior to synapse formation. *Neuron* 36: 1051–1061, 2002.
- Devor A, Fritschy JM, Yarom Y. Spatial distribution and subunit composition of GABA_A receptors in the inferior olivary nucleus. *J Neurophysiol* 85: 1686–1696, 2001.
- Dunning DD, Hoover CL, Soltesz I, Smith MA, O’Dowd DK. GABA_A receptor-mediated miniature postsynaptic currents and α -subunit expression in developing cortical neurons. *J Neurophysiol* 82: 3286–3297, 1999.
- Dzhala VI, Staley KJ. Excitatory actions of endogenously released GABA contribute to initiation of ictal epileptiform activity in the developing hippocampus. *J Neurosci* 23: 1840–1846, 2003.
- Glykys J, Mann EO, Mody I. Which GABA_A receptor subunits are necessary for tonic inhibition in the hippocampus? *J Neurosci* 28: 1421–1426, 2008.
- Glykys J, Mody I. Activation of GABA_A receptors: views from outside the synaptic cleft. *Neuron* 56: 763–770, 2007.
- Grantyn R, Henneberger C, Jüttner R, Meier JC, Kirischuk S. Functional hallmarks of GABAergic synapse maturation and the diverse roles of neurotrophins. *Front Cell Neurosci* 5: 13, 2011.
- Harvey AS, Berkovic SF, Wrennall JA, Hopkins IJ. Temporal lobe epilepsy in childhood: clinical, EEG, and neuroimaging findings and syndrome classification in a cohort with new-onset seizures. *Neurology* 49: 960–968, 1997.
- Herd MB, Brown AR, Lambert JJ, Belelli D. Extrasynaptic GABA_A receptors couple presynaptic activity to postsynaptic inhibition in the somatosensory thalamus. *J Neurosci* 33: 14850–14868, 2013.
- Hollrigel GS, Soltesz I. Slow kinetics of miniature IPSCs during early postnatal development in granule cells of the dentate gyrus. *J Neurosci* 17: 5119–5128, 1997.
- Huguenard JR, McCormick DA. Thalamic synchrony and dynamic regulation of global forebrain oscillations. *Trends Neurosci* 30: 350–356, 2007.
- Huguenard JR, Prince DA. Intrathalamic rhythmicity studied in vitro: nominal T-current modulation causes robust antioscillatory effects. *J Neurosci* 14: 5485–5502, 1994.
- Huntsman MM, Huguenard JR. Nucleus-specific differences in GABA_A-receptor-mediated inhibition are enhanced during thalamic development. *J Neurophysiol* 83: 350–358, 2000.
- Huntsman MM, Porcello DM, Homanics GE, DeLorey TM, Huguenard JR. Reciprocal inhibitory connections and network synchrony in the mammalian thalamus. *Science* 283: 541–543, 1999.
- Hutcheon B, Fritschy JM, Poulter MO. Organization of GABA receptor α -subunit clustering in the developing rat neocortex and hippocampus. *Eur J Neurosci* 19: 2475–2487, 2004.
- Jacobsen RB, Ulrich D, Huguenard JR. GABA_B and NMDA receptors contribute to spindle-like oscillations in rat thalamus in vitro. *J Neurophysiol* 86: 1365–1375, 2001.

- Jia F, Chandra D, Homanics GE, Harrison NL.** Ethanol modulates synaptic and extrasynaptic GABA_A receptors in the thalamus. *J Pharmacol Exp Ther* 326: 475–482, 2008.
- Jia F, Pignataro L, Schofield CM, Yue M, Harrison NL, Goldstein PA.** An extrasynaptic GABA_A receptor mediates tonic inhibition in thalamic VB neurons. *J Neurophysiol* 94: 4491–4501, 2005.
- Jiao Y, Sun Z, Lee T, Fusco FR, Kimble TD, Meade CA, Cuthbertson S, Reiner A.** A simple and sensitive antigen retrieval method for free-floating and slide-mounted tissue sections. *J Neurosci Methods* 93: 149–162, 1999.
- Kaneda M, Farrant M, Cull-Candy SG.** Whole-cell and single-channel currents activated by GABA and glycine in granule cells of the rat cerebellum. *J Physiol* 485: 419–435, 1995.
- Kang JQ, Macdonald RL.** The GABA_A receptor $\gamma 2$ subunit R43Q mutation linked to childhood absence epilepsy and febrile seizures causes retention of $\alpha 1\beta 2\gamma 2S$ receptors in the endoplasmic reticulum. *J Neurosci* 24: 8672–8677, 2004.
- Khalilov I, Holmes GL, Ben Ari Y.** In vitro formation of a secondary epileptogenic mirror focus by interhippocampal propagation of seizures. *Nat Neurosci* 6: 1079–1085, 2003.
- Leresche N, Lambert RC, Errington AC, Crunelli V.** From sleep spindles of natural sleep to spike and wave discharges of typical absence seizures: is the hypothesis still valid? *Pflügers Arch* 463: 201–212, 2012.
- LoTurco JJ, Owens DF, Heath MJ, Davis MB, Kriegstein AR.** GABA and glutamate depolarize cortical progenitor cells and inhibit DNA synthesis. *Neuron* 15: 1287–1298, 1995.
- Low K, Crestani F, Keist R, Benke D, Brunig I, Benson JA, Fritschy JM, Rulicke T, Bluethmann H, Mohler H, Rudolph U.** Molecular and neuronal substrate for the selective attenuation of anxiety. *Science* 290: 131–134, 2000.
- Luscher B, Keller CA.** Regulation of GABA_A receptor trafficking, channel activity, and functional plasticity of inhibitory synapses. *Pharmacol Ther* 102: 195–221, 2004.
- Macdonald RL, Olsen RW.** GABA_A receptor channels. *Annu Rev Neurosci* 17: 569–602, 1994.
- Maguire JL, Stell BM, Rafizadeh M, Mody I.** Ovarian cycle-linked changes in GABA_A receptors mediating tonic inhibition alter seizure susceptibility and anxiety. *Nat Neurosci* 8: 797–804, 2005.
- Maljevic S, Krampfl K, Cobilanschi J, Tilgen N, Beyer S, Weber YG, Schlesinger F, Ursu D, Melzer W, Cossette P, Bufler J, Lerche H, Heils A.** A mutation in the GABA_A receptor $\alpha 1$ -subunit is associated with absence epilepsy. *Ann Neurol* 59: 983–987, 2006.
- Maric D, Maric I, Wen X, Fritschy JM, Sieghart W, Barker JL, Serafini R.** GABA_A receptor subunit composition and functional properties of Cl⁻ channels with differential sensitivity to zolpidem in embryonic rat hippocampal cells. *J Neurosci* 19: 4921–4937, 1999.
- Marini C, Harkin LA, Wallace RH, Mulley JC, Scheffer IE, Berkovic SF.** Childhood absence epilepsy and febrile seizures: a family with a GABA_A receptor mutation. *Brain* 126: 230–240, 2003.
- McKernan RM, Whiting PJ.** Which GABA_A receptor subtypes really occur in the brain? *Trends Neurosci* 19: 139–143, 1996.
- Mody I, Pearce RA.** Diversity of inhibitory neurotransmission through GABA_A receptors. *Trends Neurosci* 27: 569–575, 2004.
- Mohler H.** GABA_A receptor diversity and pharmacology. *Cell Tissue Res* 326: 505–516, 2006.
- Nusser Z, Mody I.** Selective modulation of tonic and phasic inhibitions in dentate gyrus granule cells. *J Neurophysiol* 87: 2624–2628, 2002.
- Okada M, Onodera K, Van Renterghem C, Sieghart W, Takahashi T.** Functional correlation of GABA_A receptor α subunits expression with the properties of IPSCs in the developing thalamus. *J Neurosci* 20: 2202–2208, 2000.
- Pangratz-Fuehrer S, Rudolph U, Huguenard JR.** Giant spontaneous depolarizing potentials in the developing thalamic reticular nucleus. *J Neurophysiol* 97: 2364–2372, 2007.
- Pearce RA.** Physiological evidence for two distinct GABA_A responses in rat hippocampus. *Neuron* 10: 189–200, 1993.
- Peden DR, Petitjean CM, Herd MB, Durakoglugil MS, Rosahl TW, Wafford K, Homanics GE, Belelli D, Fritschy JM, Lambert JJ.** Developmental maturation of synaptic and extrasynaptic GABA_A receptors in mouse thalamic ventrobasal neurones. *J Physiol* 586: 965–987, 2008.
- Peng Z, Hauer B, Mihalek RM, Homanics GE, Sieghart W, Olsen RW, Houser CR.** GABA_A receptor changes in δ subunit-deficient mice: altered expression of $\alpha 4$ and $\gamma 2$ subunits in the forebrain. *J Comp Neurol* 446: 179–197, 2002.
- Pinault D, O'Brien TJ.** Cellular and network mechanisms of genetically-determined absence seizures. *Thalamus Relat Syst* 3: 181–203, 2005.
- Porcello DM, Huntsman MM, Mihalek RM, Homanics GE, Huguenard JR.** Intact synaptic GABAergic inhibition and altered neurosteroid modulation of thalamic relay neurons in mice lacking delta subunit. *J Neurophysiol* 89: 1378–1386, 2003.
- Poulter MO, Barker JL, O'Carroll AM, Lolait SJ, Mahan LC.** Differential and transient expression of GABA_A receptor α -subunit mRNAs in the developing rat CNS. *J Neurosci* 12: 2888–2900, 1992.
- Pritchett DB, Seeburg PH.** γ -Aminobutyric acid_A receptor $\alpha 5$ -subunit creates novel type II benzodiazepine receptor pharmacology. *J Neurochem* 54: 1802–1804, 1990.
- Rovo Z, Matyas F, Bartho P, Slezia A, Lecci S, Pellegrini C, Astori S, David C, Hangya B, Luthi A, Acsady L.** Phasic, nonsynaptic GABA_A receptor-mediated inhibition entrains thalamocortical oscillations. *J Neurosci* 34: 7137–7147, 2014.
- Rudolph U, Mohler H.** Analysis of GABA_A receptor function and dissection of the pharmacology of benzodiazepines and general anesthetics through mouse genetics. *Annu Rev Pharmacol Toxicol* 44: 475–498, 2004.
- Rula EY, Lagrange AH, Jacobs MM, Hu N, Macdonald RL, Emeson RB.** Developmental modulation of GABA_A receptor function by RNA editing. *J Neurosci* 28: 6196–6201, 2008.
- Schofield CM, Huguenard JR.** GABA affinity shapes IPSCs in thalamic nuclei. *J Neurosci* 27: 7954–7962, 2007.
- Sebe JY, Looke-Stewart EC, Estrada RC, Baraban SC.** Robust tonic GABA currents can inhibit cell firing in mouse newborn neocortical pyramidal cells. *Eur J Neurosci* 32: 1310–1318, 2010.
- Semyanov A, Walker MC, Kullmann DM, Silver RA.** Tonic active GABA_A receptors: modulating gain and maintaining the tone. *Trends Neurosci* 27: 262–269, 2004.
- Seymour VA, Everitt AB, Tierney ML.** Differential drug responses on native GABA_A receptors revealing heterogeneity in extrasynaptic populations in cultured hippocampal neurons. *J Membr Biol* 227: 111–122, 2009.
- Sigworth FJ, Sine SM.** Data transformations for improved display and fitting of single-channel dwell time histograms. *Biophys J* 52: 1047–1054, 1987.
- Sipila ST, Voipio J, Kaila K.** GAT1 acts to limit a tonic GABA_A current in rat CA3 pyramidal neurons at birth. *Eur J Neurosci* 25: 717–722, 2007.
- Sohal VS, Huguenard JR.** Inhibitory interconnections control burst pattern and emergent network synchrony in reticular thalamus. *J Neurosci* 23: 8978–8988, 2003.
- Sohal VS, Huntsman MM, Huguenard JR.** Reciprocal inhibitory connections regulate the spatiotemporal properties of intrathalamic oscillations. *J Neurosci* 20: 1735–1745, 2000.
- Stell BM, Brickley SG, Tang CY, Farrant M, Mody I.** Neuroactive steroids reduce neuronal excitability by selectively enhancing tonic inhibition mediated by delta subunit-containing GABA_A receptors. *Proc Natl Acad Sci USA* 100: 14439–14444, 2003.
- Stell BM, Mody I.** Receptors with different affinities mediate phasic and tonic GABA_A conductances in hippocampal neurons. *J Neurosci* 22: RC223, 2002.
- Studer R, von Boehmer L, Haeggi T, Schweizer C, Benke D, Rudolph U, Fritschy JM.** Alteration of GABAergic synapses and gephyrin clusters in the thalamic reticular nucleus of GABA_A receptor $\alpha 3$ subunit-null mice. *Eur J Neurosci* 24: 1307–1315, 2006.
- Swann JW.** The effects of seizures on the connectivity, and circuitry of the developing brain. *Ment Retard Dev Disabil Res Rev* 10: 96–100, 2004.
- Tan HO, Reid CA, Single FN, Davies PJ, Chiu C, Murphy S, Clarke AL, Dibbens L, Krestel H, Mulley JC, Jones MV, Seeburg PH, Sakmann B, Berkovic SF, Sprengel R, Petrou S.** Reduced cortical inhibition in a mouse model of familial childhood absence epilepsy. *Proc Natl Acad Sci USA* 104: 17536–17541, 2007.
- Vicini S, Ferguson C, Prybylowski K, Kralic J, Morrow AL, Homanics GE.** GABA_A receptor $\alpha 1$ subunit deletion prevents developmental changes of inhibitory synaptic currents in cerebellar neurons. *J Neurosci* 21: 3009–3016, 2001.
- von Krosigk M, Bal T, McCormick DA.** Cellular mechanisms of a synchronized oscillation in the thalamus. *Science* 261: 361–364, 1993.
- Wafford KA, van Niel MB, Ma QP, Horridge E, Herd MB, Peden DR, Belelli D, Lambert JJ.** Novel compounds selectively enhance δ subunit containing GABA_A receptors and increase tonic currents in thalamus. *Neuropharmacology* 56: 182–189, 2009.
- Wall MJ, Usowicz MM.** Development of action potential-dependent and independent spontaneous GABA_A receptor-mediated currents in granule cells of postnatal rat cerebellum. *Eur J Neurosci* 9: 533–548, 1997.

- Wallace RH, Marini C, Petrou S, Harkin LA, Bowser DN, Panchal RG, Williams DA, Sutherland GR, Mulley JC, Scheffer IE, Berkovic SF. Mutant GABA_A receptor $\gamma 2$ -subunit in childhood absence epilepsy and febrile seizures. *Nat Genet* 28: 49–52, 2001.
- Warren RA, Jones EG. Maturation of neuronal form and function in a mouse thalamo-cortical circuit. *J Neurosci* 17: 277–295, 1997.
- Wisden W, Laurie DJ, Monyer H, Seeburg PH. The distribution of 13 GABA_A receptor subunit mRNAs in the rat brain. I. Telencephalon, diencephalon, mesencephalon. *J Neurosci* 12: 1040–1062, 1992.
- Yu W, Jiang M, Miralles CP, Li RW, Chen G, de Blas AL. Gephyrin clustering is required for the stability of GABAergic synapses. *Mol Cell Neurosci* 36: 484–500, 2007.
- Zarnowska ED, Keist R, Rudolph U, Pearce RA. GABA_A receptor $\alpha 5$ subunits contribute to GABA_A^{slow} synaptic inhibition in mouse hippocampus. *J Neurophysiol* 101: 1179–1191, 2009.
- Zhang G, Raol YH, Hsu FC, Coulter DA, Brooks-Kayal AR. Effects of status epilepticus on hippocampal GABA_A receptors are age-dependent. *Neuroscience* 125: 299–303, 2004.
- Zhu G, Yoshida S, Migita K, Yamada J, Mori F, Tomiyama M, Wakabayashi K, Kanematsu T, Hirata M, Kaneko S, Ueno S, Okada M. Dysfunction of extrasynaptic GABAergic transmission in phospholipase C-related, but catalytically inactive protein 1 knockout mice is associated with an epilepsy phenotype. *J Pharmacol Exp Ther* 340: 520–528, 2012.

